

## Research Article

# Laboratory Experiments on Breaching Characteristics of Natural Dams on Sloping Beds

Xiangang Jiang <sup>1,2</sup>

<sup>1</sup>School of Civil Engineering, Sichuan Agricultural University, Dujiangyan 611830, China

<sup>2</sup>Sichuan Higher Education Engineering Research Center for Disaster Prevention and Mitigation of Village Construction, Sichuan Agricultural University, Dujiangyan 611830, China

Correspondence should be addressed to Xiangang Jiang; [jxgjim@163.com](mailto:jxgjim@163.com)

Received 23 July 2019; Revised 12 August 2019; Accepted 20 August 2019; Published 20 October 2019

Academic Editor: Chiara Bedon

Copyright © 2019 Xiangang Jiang. This is an open access article distributed under the Creative Commons Attribution License, which permits unrestricted use, distribution, and reproduction in any medium, provided the original work is properly cited.

Natural dams formed by landslides may produce disastrous floods after dam outburst. However, studies on the breaching characteristics of natural dams on sloping beds systematically are still at an early stage, and especially the relationship between breach width and depth is still unclear. In this paper, results of a series of laboratory tests that assessed seven different flume bed slope angles are presented. The results show that 3 stages of breaching process of natural dams on different bed slopes were observed. According to the results, headward erosion was the main force for enlargement of breach when bed slope was relatively small. With the increasing of bed slope, the effect of tractive erosion on longitudinal development of breach was enhanced. The discharge hydrographs were unimodal for all the bed slopes. The peak discharge increased first and then decreased with the increasing of bed slope. The elapsed time from the start of breach formation to the moment of peak discharge decreased with the increasing of bed slope. The difference between different bed slopes was larger when the bed slope was small or large, and the relationship between duration and bed slope had the same characteristics. With the increasing of bed slope, the ratio of breach width to breach depth rose to 1 and then decreased with the increasing of bed slope angle. A result of the present work is a function of the relationship between the breach width and depth for which it is possible to calculate them. This function is based on a shape parameter that linearly decreases with bed slope. The relationship between shape parameter and bed slope was developed to calculate the shape parameter with an additional relationship between shape parameter and mean diameter of particles. Combined with the experimental data and filed data of Tangjiashan natural dam, the shape parameter was calculated, and the function was validated.

## 1. Introduction

Excessive rainfall and earthquakes often cause landslide, which can fall into river channels and block the river. This is called a natural dam [1]. More than 50% of natural dams failed by overtopping, and 85% failed within 1 yr of formation [2]. Hazardous flooding may occur after failure of the dams. For example, in 1786, the natural dam in Dadu River failed and caused a severe flood, killing 100,000 people [3].

Many researchers investigated the field and selected data about the natural dam, such as dam height, dam width, dam volume, and so on. And then, dataset about natural dams were primarily established. For example, Eisbacher and

Clague, Pirocchi, and Casagli and Ermini investigated natural dams in Alpine mountains [4–6]; Costa and Schuster collected 460 natural dams' data worldwide [2]; Clague and Evans included landslide dams from the Canadian cordillera [7]; Chai et al. included 147 landslide dams from China [8]; Peng and Zhang collected 1239 landslide dam cases and developed a database [9]; and some famous landslide dams occurred recent years [10–14]. Data are derived from the cases inventoried by the authors and from cases collected from review work. These data mainly include the height, width, length, area, and volume of natural dams. With these data, some qualitative analysis could be carried out, such as the safety of natural dams could be evaluated with geomorphologic factors based on an analysis of 84 episodes of

selected natural dams worldwide [15]; and breaching parameters could be predicated with some field data [10, 16]. However, few breaching photographs, videos, and field data were recorded when natural dams failed by limited observation technology. In such way, the characteristics of breaching for natural dams, especially the overtopping mode, are not able to make clear with above-mentioned field data.

The size of the breach and the magnitude of the resulting flood are controlled by many factors, which include geomorphological factors, e.g., bed slope and dam's geometry, sediment characteristics, and so on. Many researchers have studied the influence of dam's geometry on failure process and discharge hydrograph and found a steeper downstream slope of dam could result in a larger peak discharge and shorter duration [17–20]. The breaching process may differ notably due to different compositions of fine and coarse particles. And, the fines contents or median diameter of the dam materials have an important effect on the discharge [17, 18, 21–26]. The rate of inflow could also change the erosion process during the failure process and then affect the breach development and outflow [19, 27]. However, there are few studies about influence of bed slope on breaching characteristics of natural dams until now.

The breaching characteristics of natural dams include both the evolution of breaching discharge and spatial evolution of breach. The evolution characteristics of breach discharge mainly include characteristics of discharge hydrographs, peak discharge, and breaching time. The evolutionary characteristics of breach mainly entail variation of breaching depth and width. However, at present, the process of breaching discharge has been studied separately from the characteristics of breach [18, 24, 28], so thorough analysis about the breaching characteristics by considering these two aspects comprehensively have failed.

The breach development is actually the relationship between breach width and depth. Because of the limitations of observation technology, the existing research can hardly confirm the quantitative relationship between breach depth and width, leaving a research gap. Although Coleman et al. proved that the breach shape can be described by a parabolic equation through experimental observation [17], the case is different from natural dams. Pickert et al. and Do et al. obtained breach longitudinal and transverse profiles at different stages, but the definite relationships between the two directions are unclear [23, 29]. Zhu et al. studied in detail the variation of breach longitudinal profiles, but the regularities of breach widening have not been studied [30].

In field, the natural dam could block river and gully. The bed of river is usually gentle, and the bed of gully is steep. In this paper, the bed slope was designed from  $1^\circ$  to  $13^\circ$  to simulate natural dams located in both river and gully. This paper aims to improve the understanding of influence of bed slope on breaching characteristics of natural dams triggered by overtopping. In this paper, a series of flume tests to study the breaching characteristics of natural dams on sloping beds are presented. Firstly, the influences of bed slope angles on breach discharge

hydrograph, peak discharge, time to peak discharge, duration, breach depth, and breach width are analyzed. Then, the relationship between breach width and depth is discussed. In the end, the relationships between parameters in the breach width-depth function and bed slope are investigated.

## 2. Experimental Setup and Procedure

*2.1. Experimental Prototype and Materials.* The experimental models are based on the Zongqu natural dam prototype. The Zongqu natural dam was formed after Wenchuan earthquake and overtopped in 2009 [31]. The Zongqu gully is located about 7 km in the south of Maoxian County, Sichuan province, which is a primary tributary on the left bank of Minjiang River. The entire basin is located in the southeast of Sichuan Plateau (Figure 1). The longitudinal section of Zongqu natural dam is similar to the shape of a trapezoid. The top crest width and the height of the dam were both approximately 30 m. The length across the river was approximately 60 m. The bed slope was approximately  $4^\circ$  at the location of the natural dam. The upstream and downstream slopes of the dam were approximately  $34^\circ$  and  $17^\circ$ , respectively. The materials in the dam were block rocks, gravels, sand, silt, and clay. The content of block rocks with diameters of 100–300 cm was approximately 5%. The content of particles 30–100 cm in diameter was approximately 60%, and 35% of particles had a diameter less than 30 cm. We set the length ratio  $\lambda_L = 1 : 100$  in the present models. The experimental material with a diameter of 1–3 cm was 5%, 0.3–1 cm was approximately 60%, and less than 0.3 cm was about 35%. In addition, to avoid the influence of viscosity of flow on the breaching process, the content of clay particles should not be large. The content of clay particles was 1.872% in the present models. The median diameter  $D_{50}$  was 0.48 cm. The initial dry density was  $1.72 \text{ g/cm}^3$ . The grain-size distribution curve of the experimental materials is shown in Figure 2. Before each test run, we weighed approximately 300 kg of material that fits the gradation curve and watered the composition.

*2.2. Experimental Setup.* Based on the length ratio  $\lambda_L$ , the dam crest width and height were both 30 cm for the experimental models. Natural dam breaching is a free water surface process dominated by gravity, followed the Froude principle. If  $\lambda_L$  is scale ratio, based on the Froude number  $F = v/(gL)^{0.5}$ , with  $v$  being the velocity,  $g$  being the gravity acceleration, and  $L$  being the length, the scale ratio for inflow discharge is  $\lambda_L^{0.5}$ . Based on small watershed convergence model, reasoning formula method was used to calculate the designed inflow rate of Zongqu watershed. The characteristic value of catchment area of the basin was taken from the area above Zongqu natural dam by a topographic map of 1 : 50000; the catchment area was  $15 \text{ km}^2$ , and the main channel length was 7.5 km. The confluence parameters, designed storm value, etc., were obtained according to the Handbook for Calculation of Storm Floods in the Medium and Small Watersheds of Sichuan Province [32]. When design frequency was 2%, the calculated

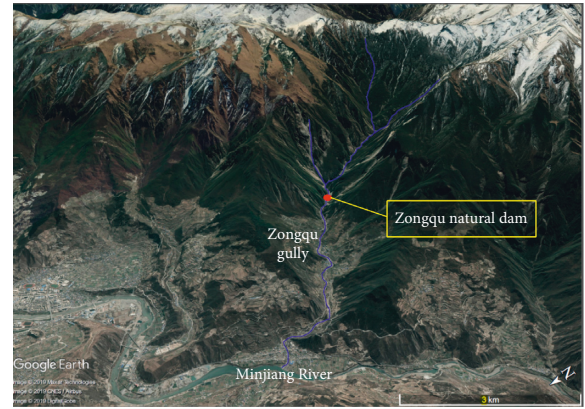
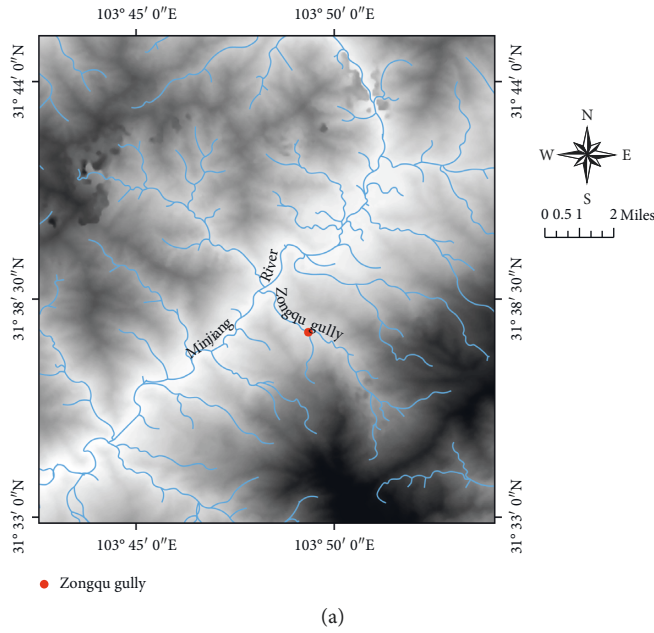


FIGURE 1: Location of the Zongqu gully and Zongqu natural dam. (a) Location of the Zongqu gully (b) Location of the Zongqu natural dam in the gully.

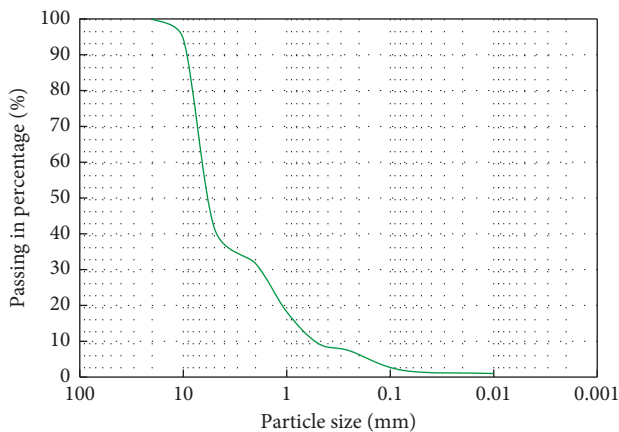


FIGURE 2: Particle size distribution of the material.

peak discharge at the section of the dam was set as actual inflow rate of Zongqu natural dam. Therefore, the discharge ratio  $\lambda_Q = \lambda_L^{2.5} = 1 : 100000$ , and the inflow rate in the tests was about 1.0 L/s.

A half-width of dam was chosen and scaled down with  $\lambda_L$ . The initial breach was beside the flume wall, assuming a little effect of the flume sidewall on the breach flow and a symmetric breach advance (Figure 3). It is noted that very small flow depths with low Reynolds number might generate some delay in the breach discharge due to viscous and capillarity effects at the interfaces of glass/water and grain/water up to the point at which a turbulent flow is fully developed at the beginning of overtopping. However, these effects have minor importance due to the fast increasing breach discharge [23]. This assumption is supported by the findings of Schmocker and Hager [28] for small-scale models [23].

The experiments were carried out in a 15 m long, 0.3 m wide, and 0.6 m deep flume, and the adjustable slope angle was 0–30°. The flume was made of tempered glass to clearly see the breach bottom during the breaching process. The width of the dam crest  $W$  and initial dam height  $H_b$  were both 30 cm. We preset an initial triangular breach at one side of the dam. Both of its depth and width were 4 cm (Figure 3). The inflow discharge was accurately controlled by an electromagnetic flowmeter. The tests involved the use of a movable riverbed with thickness of 5 cm, which was made of the same materials with the dam. As the boundary condition, a plate with a height of 5 cm was set at the end of the flume. In the experiments, the upstream slope toe of the dam was set up at a distance of 10 m from the intank. The experimental setup is shown in Figure 3.

For the first test, we set the flume bed slope as 1°, and the upstream and downstream slopes of the dam were set as 30° and 20°, respectively.  $\theta$  is the flume slope, and  $\beta$  is the downstream slope of the dam. Then, other six tests with flume bed slope of 2°, 3°, 7°, 9°, 11°, and 13° were set, whose other conditions except lake volume before the dam were the same with the first test.

A piezometer was buried in front of the dam. The piezometer recorded the depth of water upstream of the dam, and the data were collected by a computer automatically.

**2.3. Measurements.** The upstream water pressure could be recorded by the piezometer set at the upstream of the dam. According to the principle of hydrostatic pressure, the water level in front of the dam could be converted by the water pressure, and the breaching discharge in the failure process was calculated based on the water balance equation:

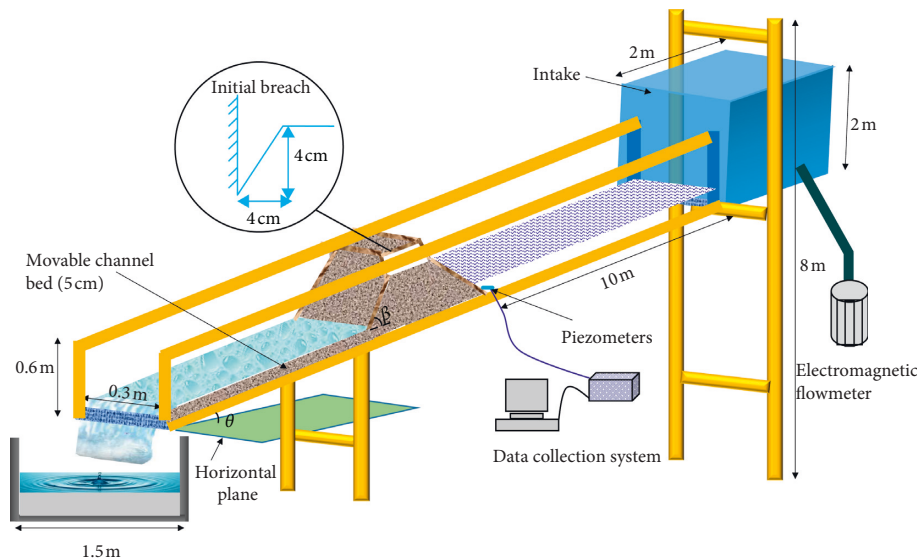


FIGURE 3: A sketch of the flume and its hydrological equipment. It shows the full size and shape of the dam and the size of the initial breach.

$$Q = q_{in} - \frac{dW}{dt}, \quad (1)$$

where  $Q$  is the outflow discharge, L/s;  $q_{in}$  is the inflow discharge, L/s;  $t$  is time, s; and  $W$  is the volume of reservoir as a function of water surface elevation.

Cameras were set in different places around the dam. A grid paper was set on the side glass of the flume to measure the height of the breach bottom. The accuracy of the measurement reached 5 mm. Combining the measured height of the breach bottom and the initial dam height, the breach depth could be determined.

### 3. Experimental Results

**3.1. General Features.** The results show that the breaching characters of dams in the tests, which included outflow characters, erosion characters, and breach enlargement characters, were similar. And, the overtopping process of all experiments had three same phases. At the first stage (0- $t_1$ ), the sediment at the breach of dam crest was dominated by the suspended load movement. And, the sediments accumulated at the downstream slope and formed an obvious slope turning point. The breach slope collapsed intermittently on a small scale, and the breach shape in this stage approached to a rectangle. The slope turning point reached the intersection point of downstream slope and breach bottom when  $t = t_1$  (Figure 4(a)). At the second stage ( $t_1$ - $t_2$ ), backward erosion became serious with more water outflow. The backward erosion reached upstream slope when  $t = t_2$  (Figure 4(b)). In this stage, there were break points at downstream slope, which was the characteristic of backward erosion. The strength of erosion under the slope of the break point became slower, while the upper slope became stronger. When the slope break point moved to the upstream slope, the elevation of water upstream showed a sudden decline (Figure 4(d)). The shape of the breach was similar to a

trapezoid. The deepening and widening of breach in this stage was the most rapid one. At stage three ( $t_2$ - $t_3$ ), the outflow discharge was gradually decreased, and the water depth became shallow and sand carrying capacity was gradually weakened. And, a coarse layer which protected the lower particles from being washed away was formed (Figure 4(c)). At that moment, the motion of water and sand could reach a new balance, indicating the end of the failure process. The shape of breach was also like a trapezoid during this stage.

**3.2. Characteristics of Breach Discharge.** Figure 5 shows the discharge hydrographs of the natural dam with seven slope angles ( $1^\circ$ ,  $2^\circ$ ,  $3^\circ$ ,  $7^\circ$ ,  $9^\circ$ ,  $11^\circ$ , and  $13^\circ$ ). As is shown, in different slope conditions, the breach discharge increases as time increases and then reaches the peak discharge; subsequently, the breach discharge decreases gradually. This feature indicates that breach discharge at different slopes has strong unsteady characteristics. The figure reflects the smaller the bed slope is, the longer breaching time is, and the fatter the curve is. The peak discharge is only one for all conditions. It means that the bed slope does not change the number of peak discharge point for hydrograph.

The relationship between peak discharge and bed slope is shown in Figure 6. According to the form of the curve, peak discharge increases with the increase in slope when the slope is less than  $3^\circ$ . However, it gradually decreases when the slope is larger than  $3^\circ$ . The main reason for causing this phenomenon is that when the slope is below  $3^\circ$ , the water upstream dam is abundant for outflowing, and, the bed slope is the controlling factor for breach development. As the slope increases, the shear force of outflow is strengthened, and the breach expansion is accelerated, which causes larger outflow. Therefore, the peak discharge increases gradually along with the increase in slope. When slope becomes more than  $3^\circ$ , the pre-dam storage capacity decreases with the increase in



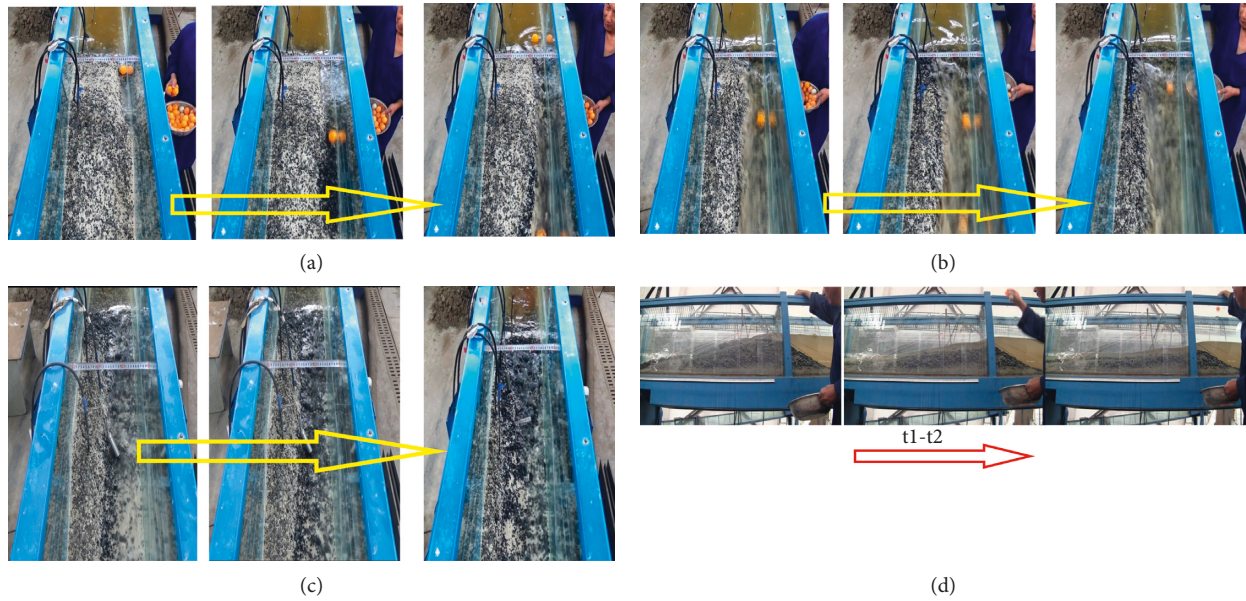
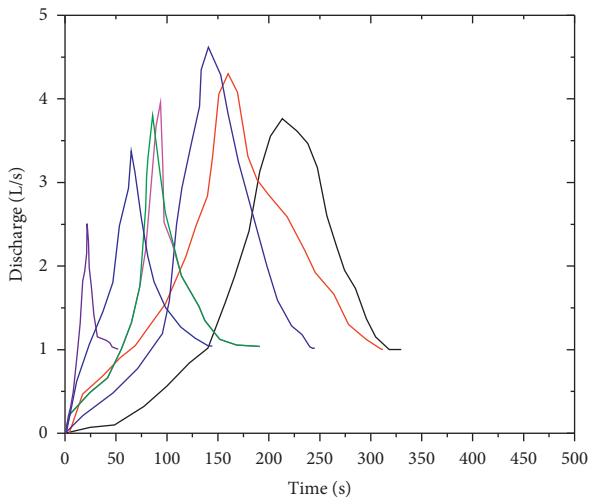


FIGURE 4: Images of dam and flow at different times, showing overtopping erosion is the dominant factor for dam failure. (a) Stage I for dam failure process, 0-t1 period. (b) Stage II for dam failure process, t1-t2 period. (c) Stage III for dam failure process, t2-t3 period. (d) The longitudinal profiles of the dam in Stage II. It shows a whole backward erosion process.



- Outflow with the channel bed slope of 1°
- Outflow with the channel bed slope of 2°
- Outflow with the channel bed slope of 3°
- Outflow with the channel bed slope of 7°
- Outflow with the channel bed slope of 9°
- Outflow with the channel bed slope of 11°
- Outflow with the channel bed slope of 13°

FIGURE 5: Breach discharge hydrographs for different channel bed slopes.

slope. Although the erosion ability is strengthened with the increase in slope, the decrease of predam storage capacity contributes to insufficient outflow discharge. This causes the decrease in peak discharge with the increase in bed slope. Thus, in this condition, predam storage capacity is the main factor that affects peak discharge. At the same time, in the

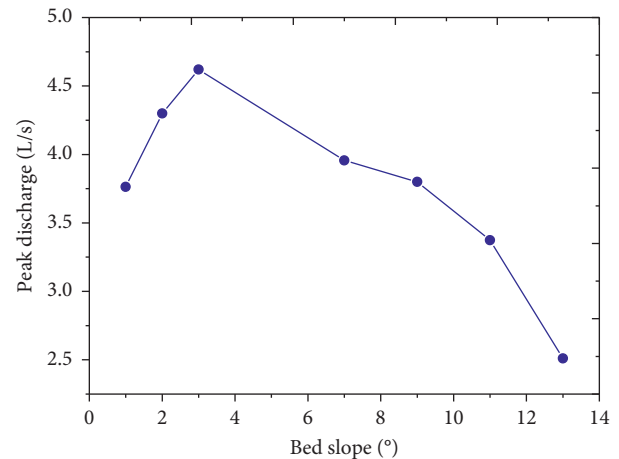


FIGURE 6: The relationship between peak discharges and bed slopes.

growth stage of peak discharge, it grows faster when slope is 2°-3° than that of 1°-2°. And, in the decreasing stage of peak discharge, it decreases faster when slope is 9°-13° than that of 3°-9°. It indicates that the steeper the slope is, the greater the increment of peak discharge in growth stage is and the decline rate of peak discharge in decrease stage is.

Figure 7 shows the bed slope could shorten the duration of hydrographs and time from test start to the moment of peak discharge. It means the larger bed slope could decrease the dam's life span and advance the peak discharge. The figure indicates that the duration and time from test start to the moment of peak discharge with the bed slope are nonlinear relationships. When bed slopes are smaller than 3° and larger than 9°, the duration and time from test start to the moment of peak discharge decrease more quickly than the others. The average reduction rate of

duration and time to peak curve are 23 s and 16 s, respectively per bed slope, indicating duration decreases more quickly than time from test start to the moment of peak discharge.

**3.3. Characteristics of Breach Development.** Figure 8 shows longitudinal profiles of natural dam with different slopes. As is shown, under different slope conditions, dam crest has different degrees of bending characteristics. Especially, after a period of breaching time, break point is formed on the dam crest, that is the symbol of headward erosion. Under different slope conditions, the failure process is basically the same, including slow overcurrent, headward erosion, and rebalance of sediment and water. Thus, it means that the variation of slope does not change characteristics of failure process. Breach longitudinal profiles in that seven slopes all show that strong headward erosion existed in stage II. The number of break point decreases as the bed slope becomes larger. Compared with the residual dam height in different slopes, as the slope increases, residual dam height decreases gradually.

Figure 9 shows the relationships between breach width and depth during failure process. It is seen that the breach width increases when the breach deepens. At the early and late stage of breach growth, the breach widens slowly. Otherwise, the breach widens rapidly, in which the curve is similar to the shape “S”. Overall, the curves of breach depth and width at any time are partly located above the straight line with a slope of  $K=1$ , when the slope is  $1^\circ\text{--}3^\circ$ . While the slope is more than  $7^\circ$ , all curves are located basically below that straight line. It indicates that during the development of breach, the breach width increases faster than depth when the slope is relatively small. Nevertheless, it is the opposite as for the steeper slopes. When the failure process is over, as slope increases, the breach width-depth graphs firstly approach the straight line with a slope of  $K=1$  and then get away from it. It indicates that the breach width-to-depth ratio increases to 1, and then decreases as the slope increases.

#### 4. Relationships between Width and Depth of Breach

Based on the experimental data, we converted breach width and depth to dimensionless values. The dimensionless breach depth  $D^*$  and width  $W^*$  are set as follows:

$$\begin{aligned} D^* &= \frac{D}{H_d}, \\ W^* &= \frac{W}{H_d}, \end{aligned} \quad (2)$$

where  $D$  (cm) and  $W$  (cm) are breach depth and width, respectively, and  $H_d$  (cm) is the dam height.

To obtain the functional relation between  $W^*$  and  $D^*$ , all the test data were fitted as shown in Figure 10. This figure shows that all the fitting curves fit the experimental data well, and the fitting curves could be expressed by the following equation:

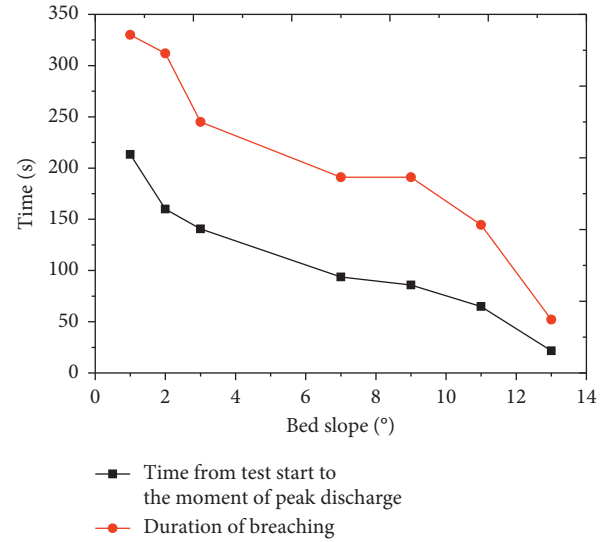


FIGURE 7: The relationship between time from test start to the moment of peak discharge and duration of hydrograph and bed slopes.

$$W^* = \frac{\eta}{1 + e^{(-k(D^* - \gamma))}}, \quad (3)$$

where  $\eta$ ,  $k$ , and  $\gamma$  are parameters. The parameter  $\eta$  reflects the possible maximum breach width;  $k$  is the shape parameter, which represents steep or gentle of the curve, reflecting growth rate of breach. If the absolute value of  $k$  is larger, the breach width increases faster. On the contrary, the width expands slower with a smaller  $k$ . The parameter  $\gamma$  reflects the corresponding depth of the breach when it reaches half of the maximum breach width.

Figure 11 shows the influence of slope on breaching parameters  $\eta$ ,  $k$ , and  $\gamma$ . It indicates that  $\eta$  increases with  $\theta$  and then decreases, but the relation between  $\gamma$  and  $\theta$  is opposite. The larger  $\theta$  is, the smaller  $k$  becomes. Furthermore, the parameters  $k$  and  $\theta$  agree with linear relationship.

#### 5. Discussion

Lang, Zhang, and Huang calculated the peak discharge and velocity at the peak discharge based on the hydrological data in the field of the Zongqu natural dam, and considered the peak discharge of  $300\text{--}600\text{ m}^3/\text{s}$  and the velocity of approximately  $34\text{ m/s}$  at the peak discharge time [33, 34]. For the experimental model with the flume bed slope of  $1^\circ$ , the peak discharge is  $3.8\text{ L/s}$ , which agrees with the field data transformed value of  $3\text{--}6\text{ L/s}$  based on the scale ratio. Meanwhile, the velocity of the outflow surface was measured to be approximately  $3.2\text{ m/s}$  at the peak discharge moment, which was approximately equal to the field data transformed value of  $3.4\text{ m/s}$  based on the scale ratio. These findings mean that the hydraulic parameters in model test are consistent with the field data. Also, it indicates that the boundary effect on the motion of outflow may not be serious in the tests. In such way, laboratory tests may model the hydraulic characteristics of the natural dam.

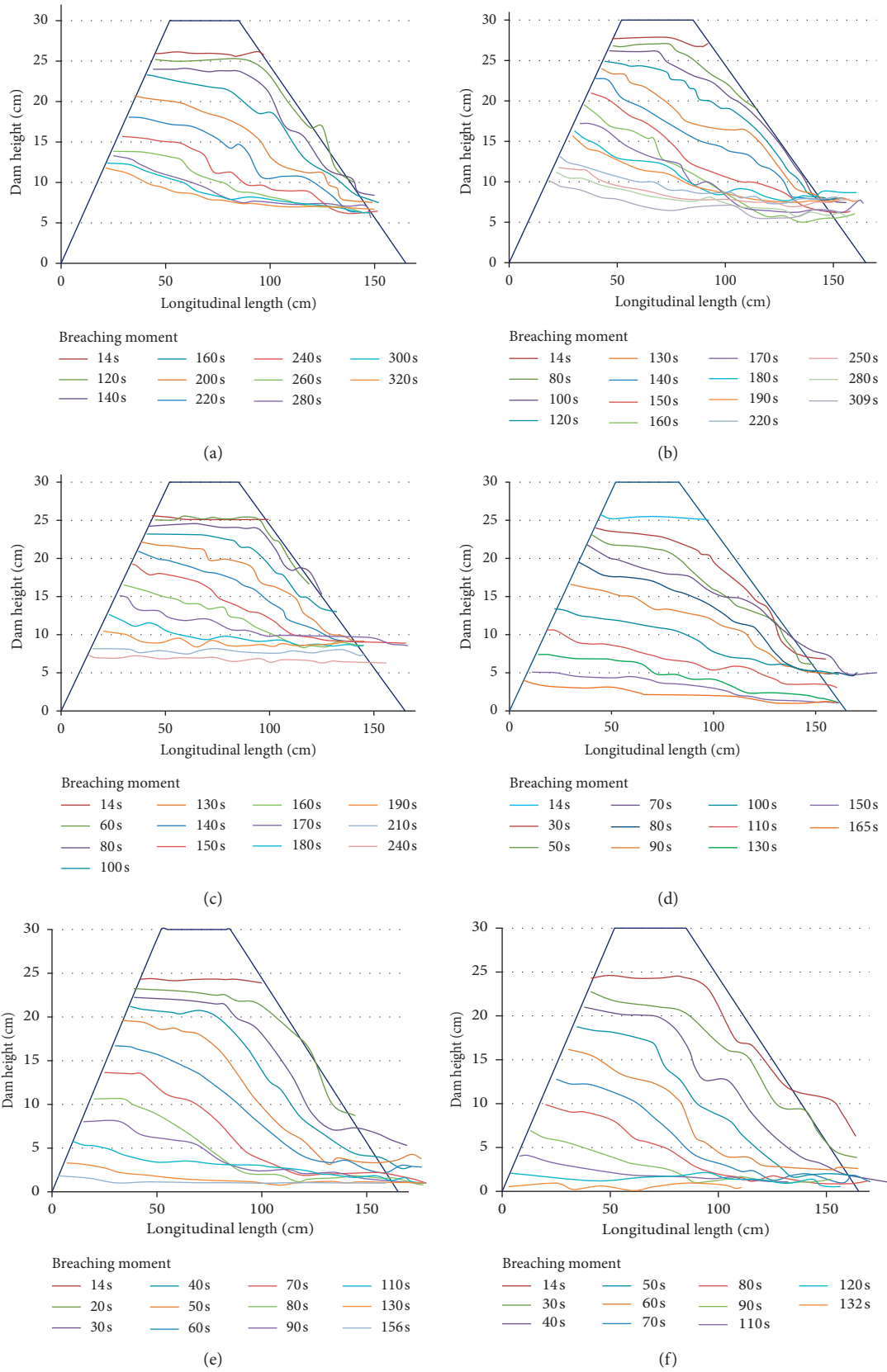


FIGURE 8: Continued.

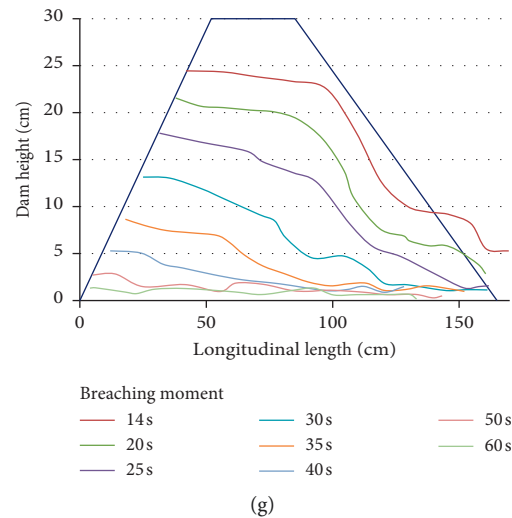


FIGURE 8: Longitudinal profiles of the dam during failure process for different channel bed slopes at different times. (a) Bed slope of  $1^\circ$ . (b) Bed slope of  $2^\circ$ . (c) Bed slope of  $3^\circ$ . (d) Bed slope of  $7^\circ$ . (e) Bed slope of  $9^\circ$ . (f) Bed slope of  $11^\circ$ . (g) Bed slope of  $13^\circ$ .

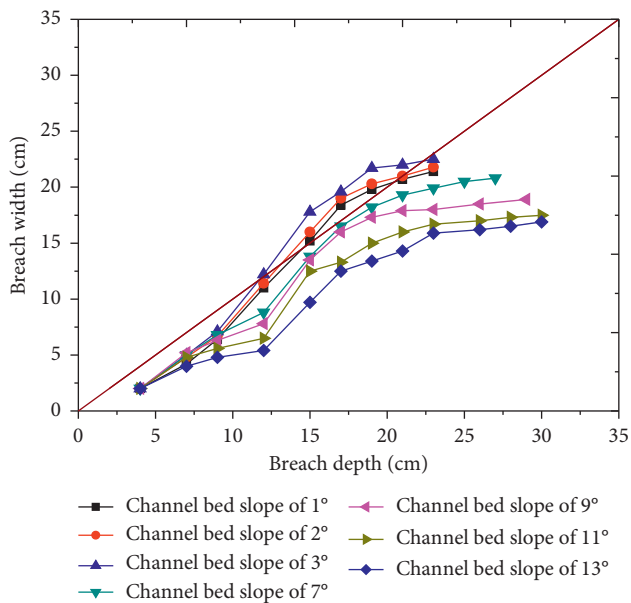


FIGURE 9: The relationship between breach width and depth for different bed slopes.

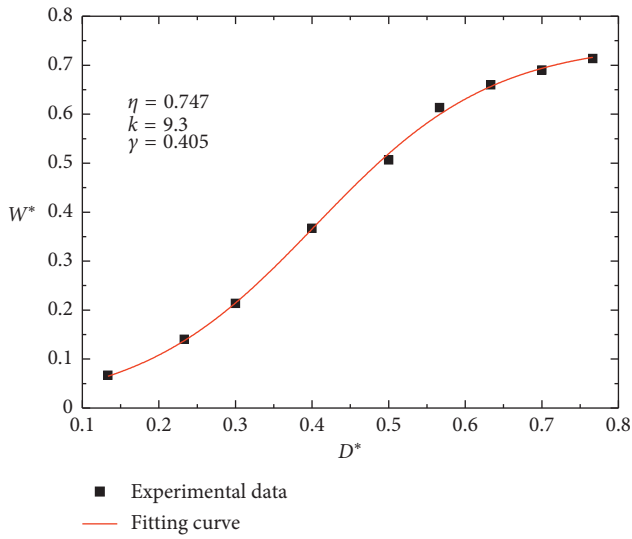
Natural dams are not only common in rivers with small bed slopes, but also in the gully with large bed slopes. Previous studies and conclusions are mostly focused on the dam failure on small bed slope. This paper shows the breaching process of natural dams on different bed slopes, especially the large bed slope. It also clearly reflects the relationship between breaching parameters and the bed slope. It should be noted that this paper just intends to study the influence of bed slope on breaching process of natural dams. However, the lake volume changes indeed when changing the bed slope and keeping the other parameters the same. It means that the bed slope of the channel could change both the topographical condition and hydraulic condition. However, the bed slope and lake

volume are dependent, and the lake volume is a function of bed slope. In this respect, the independent variable is only bed slope.

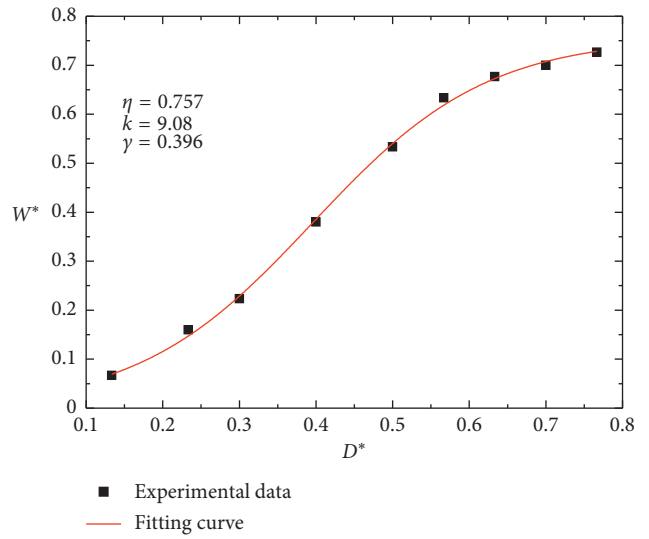
After the natural dam formation, the researchers concern the outflow peak discharge during the failure process. When analyzing the peak discharge, it is often estimated based on lake volume, which is called parameter model [35]. In general, it has a negative correlation between lake volume and bed slope. In such methods, the relationship between peak discharge and bed slope is a negative correlation. Figure 12 shows the relationship between peak discharge and bed slope for the experiments in this paper based on Evans's and Hagen's methods [36, 37]. It shows that the peak discharge decreases with the bed slope which is inconsistent with the experimental data. In addition, the calculated values are less than the experimental values. It is observed that the trend of the calculated values is similar to the experimental data when the bed slope is large, but opposite with the small bed slope. It is worth mentioning that the parameter model almost ignored the influence of bed slope on peak discharge. It does not agree well with the field situation, such as the natural dam in the gully with a large bed slope. For such a dam in gully, it should not only consider the variation of lake volume induced by bed slope but also the variation of erosion rate induced by bed slope. In such way, the results and conclusions in this paper may provide some references to peak discharge calculation for natural dam with different bed slopes.

A lot of calculation methods about discharge are related to water head and breach width [38–41]. It is obvious that the water head could be calculated if the breach bottom is known together with the water balance equation. The breach bottom is influenced by erosion only. If we know the erosion rate, the evolution characteristics of breach bottom/breach depth could be obtained. And, it is

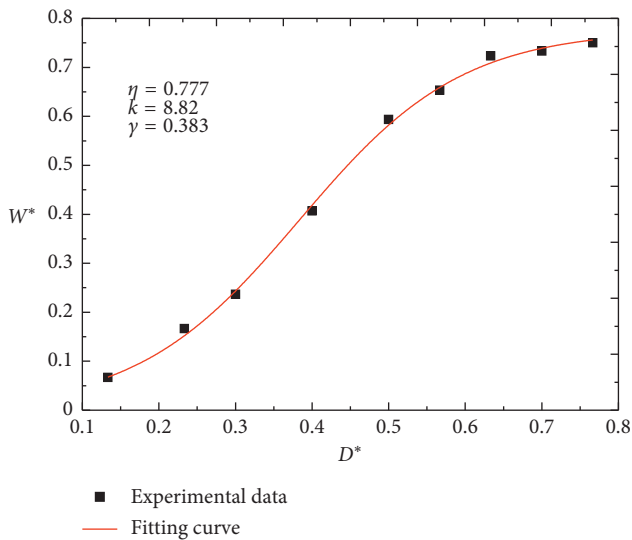




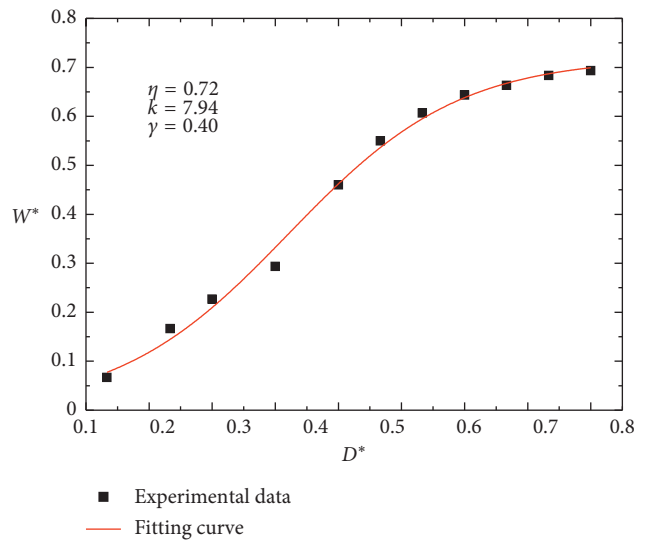
(a)



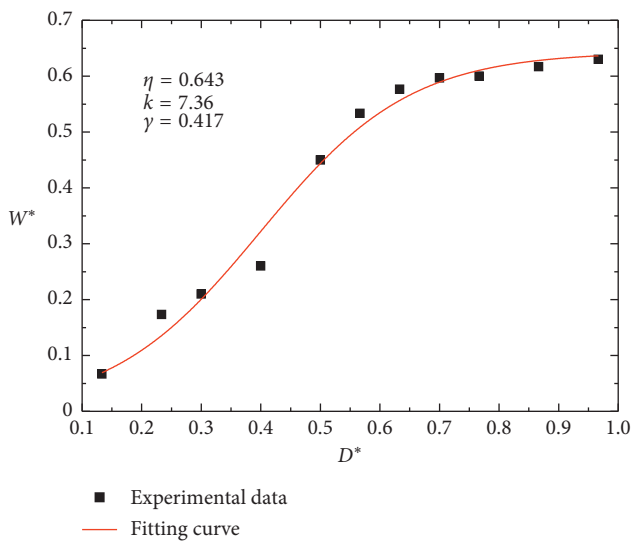
(b)



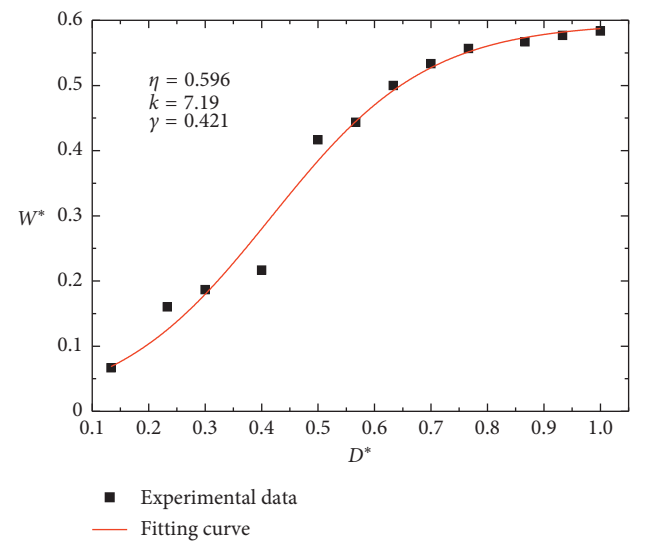
(c)



(d)

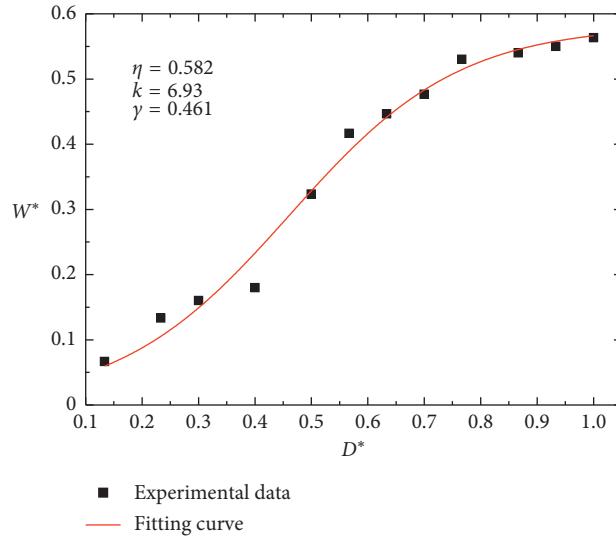


(e)



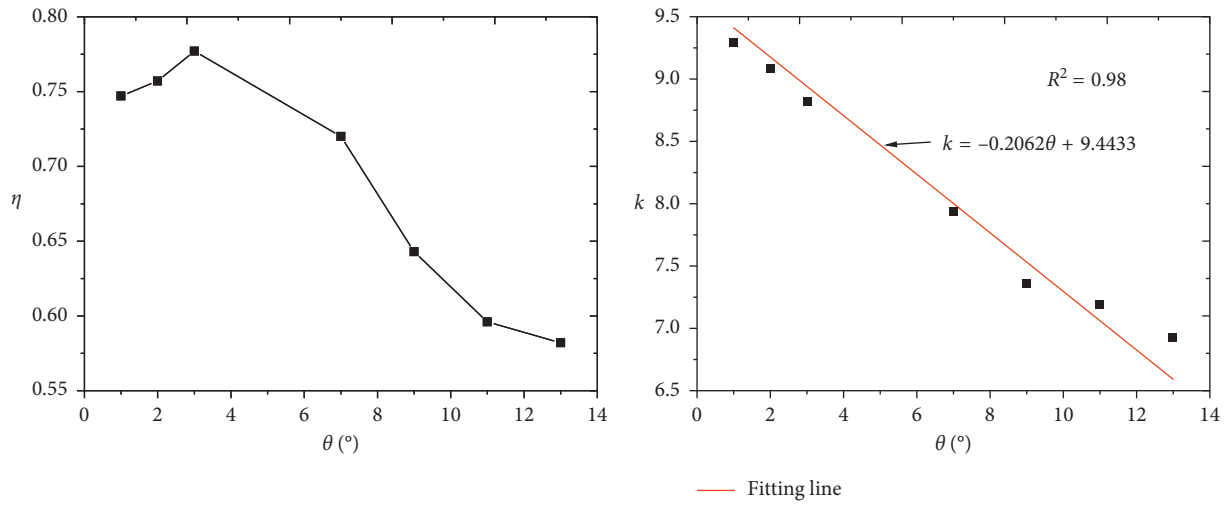
(f)

FIGURE 10: Continued.



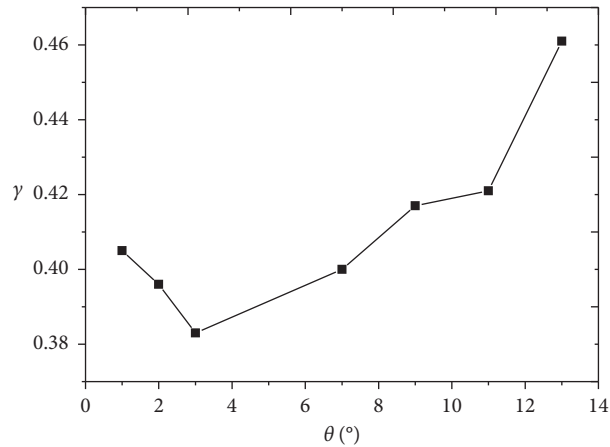
(g)

FIGURE 10: The relationship between the experimental data and fitting curves for  $W^*$  and  $D^*$ . The parameters  $\eta$ ,  $k$ , and  $\gamma$  in fitting equation (3) are shown in each figure. (a) Bed slope of  $1^\circ$ . (b) Bed slope of  $2^\circ$ . (c) Bed slope of  $3^\circ$ . (d) Bed slope of  $7^\circ$ . (e) Bed slope of  $9^\circ$ . (f) Bed slope of  $11^\circ$ . (g) Bed slope of  $13^\circ$ .



(a)

(b)



(c)

FIGURE 11: The relationships between parameters in equation (3) and bed slopes. (a) The relationship between  $\eta$  and bed slopes. (b) The relationship between  $k$  and bed slopes. (c) The relationship between  $\gamma$  and bed slopes.

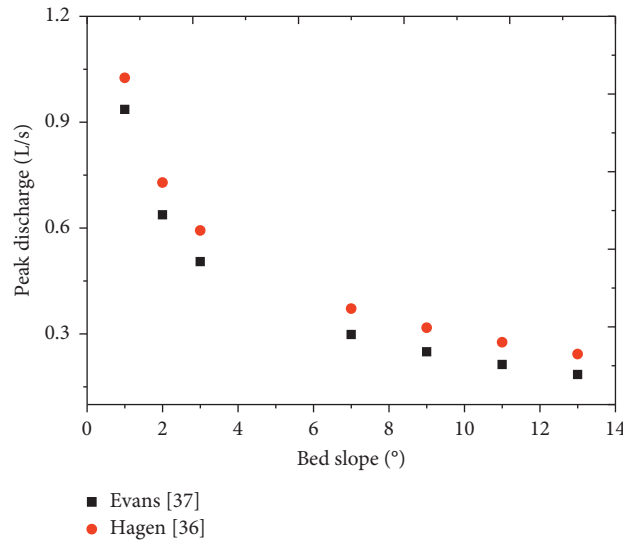


FIGURE 12: The relationship between calculated peak discharge values with Evans’s and Hagen’s methods [36, 37] and bed slopes.

not difficult to calculate the erosion rate at present. The methods for erosion rate calculation could refer to Van Rijn, Chang and Zhang, and Wu [42–44]. The breach width is an important parameter to calculate outflow discharge. The breach width is mainly caused by lateral erosion and breach side slope collapse. At present, the lateral erosion rate is assumed to be equal to the incised erosion rate. In fact, the shear stress of outflow is different along the breach. Therefore, Osman and Thorne indicated that the above assumption may be uncorrected [45]. It is noted that there is still not a calculation method of lateral erosion rate for noncohesive materials. Although many models analyzed breach slope collapse based on force equilibrium, sometimes the failure plane is not linear or circle as the assumption of models [46]. In addition, the collapse of breach side slope is random indeed in field of natural dams. In such way, the breach width calculation value may be far from the observed value based on the complex method (i.e., the addition of lateral erosion and collapse of breach side slope). Therefore, another practical and effective method may be developed avoiding calculating lateral erosion and collapse of breach side slope. Based on such thought, the relationship between breach width and depth intend to be determined. After all, the incised erosion rate is easier to obtain than the later erosion rate. Moreover, it may be a new way for getting breach width based on the breach depth which is more easy to obtain.

From the data of Jiang et al. [26], the relationship between parameter  $k$  in equation (3) and medium diameter of dam material could be obtained (Figure 13). So, the parameter  $k$  could be calculated with the relationship between  $k$  and medium diameter first and then improve the parameter with the relationship between  $k$  and bed slope. The parameter  $\eta$  reflects the maximum breach width after the dam failure. This parameter could be calculated with the method provided by Peng and Zhang [9]. The last parameter in equation (3) is  $\gamma$ . If the initial breach width and depth are

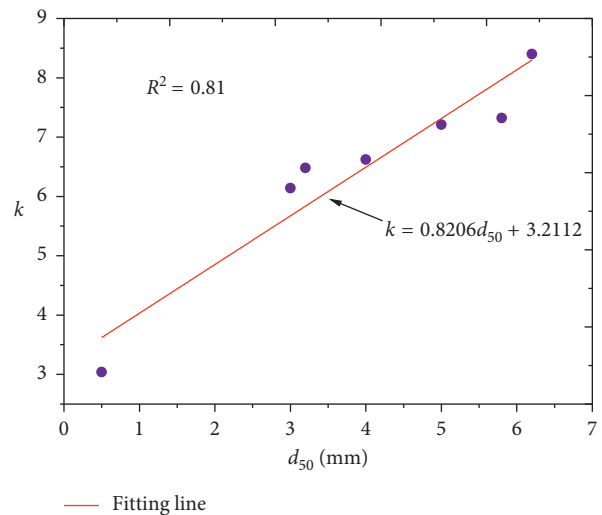


FIGURE 13: The relationship between parameter  $k$  and medium diameters. The data are from Jiang et al. [26].

given, the parameter could be calculated, and then the equation (3) is confirmed.

The formula developed in this paper, e.g., equation (3), is also validated with data provided by Coleman et al. and Pickert et al. [17, 23] (Figure 14). It is clear that the breach width and depth described in Coleman et al. and Pickert et al. also obey the formation of equation (3) [17, 23].

The Tangjiashan natural dam is the largest natural dam caused by Wenchuan earthquake. The dimensionless breach depth and width data during Tangjiashan dam failure are shown in Figure 15.

The initial breach width and depth are about 11.5 m and 10 m [47]. Firstly, based on the relationship between parameter  $k$  and medium diameter in Figure 13,  $k = 19.62$ . Then, modifying the parameter  $k$  according the relationship between  $k$  and bed slope in Figure 11(b), the final value of  $k = 18.27$  is obtained. The value of parameter  $\eta$  equals to 2.06

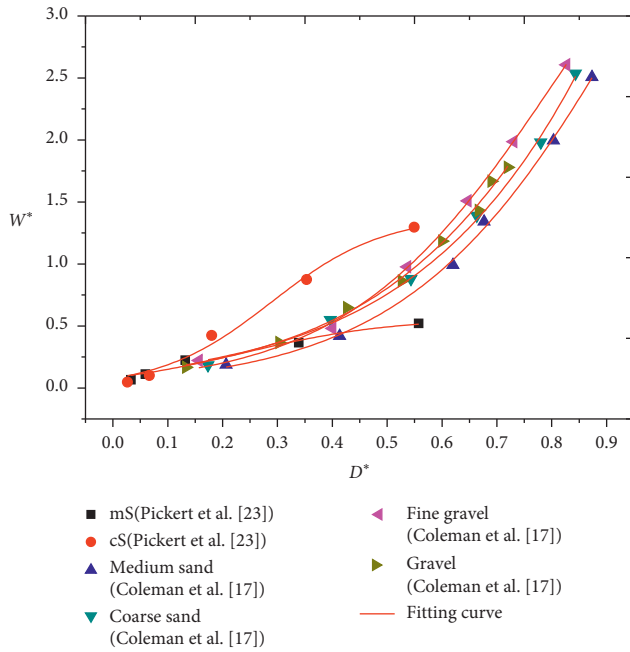


FIGURE 14: The relationships between breach width and depth in dimensionless formation. The scatter points were measured data by Coleman et al. [17] and Pickert et al. [23]. The fitting curve in the figure is analyzed based on equation (3).

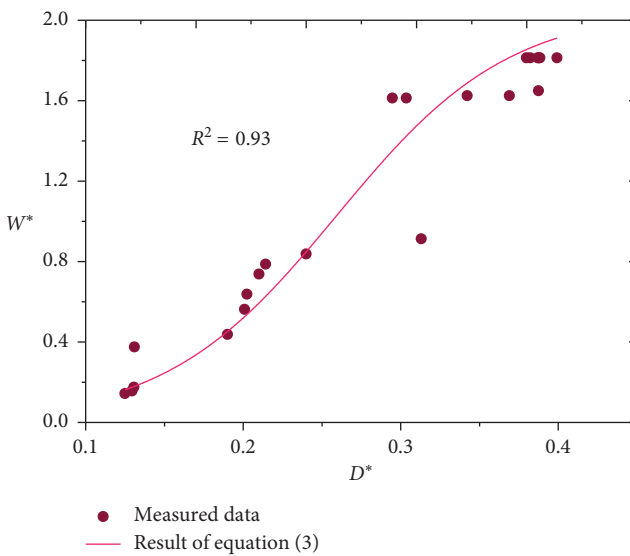


FIGURE 15: The dimensionless breach width and depth of the Tangjiashan natural dam. The points in the figure are the field data recorded during Tangjiashan natural dam failure process. The fitting curve is the simulated results of equation (3).

based on the method provided by Peng and Zhang [9]. On the basis of the initial breach width and depth of the Tangjiashan natural dam, the parameter  $\gamma$  could be calculated as 0.26 with equation (3). Figure 15 shows the results of simulated breach width and depth with equation (3). It indicates that the calculated values are close to the measured values. It proves the equation (3) is feasible to evaluate the breach size.

## 6. Conclusions

A series of tests were conducted to investigate the failure process of natural dam on sloping beds. In the present experiments, overtopping erosion was the primary mechanism of natural dam failure. The breaching process of natural dams on different sloping beds was divided into three breach phases. Headward erosion plays a dominant role during the erosion process.

The discharge hydrographs are unimodal no matter bed slope is large or not. With the increase in slope, peak discharge increases at first and then decreases while breaching time decreases gradually. The time from test start to the moment of peak discharge becomes earlier as bed slopes become bigger. The rate of decreasing for the time from test start to the moment of peak discharge and duration decreases first and then increases with the increase in bed slope.

As slope increases, breach width-to-depth ratio tends to be 1 and then to be less than 1. The breach width and depth follow a logistic equation formula. There are two parameters that could reflect the maximum breach size in the equation. Also, a shape parameter in the equation has a linear relationship with bed slope. With breaching data of experiments and Tangjiashan natural dam, it proves that the breach width and depth could be simulated well with the formula developed in this paper.

## Data Availability

The data used to support the findings of this study are available from the corresponding author upon request.

## Conflicts of Interest

The authors declare that there have no conflicts of interest.

## Acknowledgments

The authors acknowledge financial support provided by the National Natural Science Foundation of China (no. 41807289) and Sichuan Province Fundamental Scientific Research (no. 18ZA0374).

## References

- [1] T. Takahashi, *Debris Flow: Mechanics, Prediction and Countermeasures*, Taylor & Francis, London, UK, 2007.
- [2] J. E. Costa and R. L. Schuster, "The formation and failure of natural dams," *Geological Society of America Bulletin*, vol. 100, no. 7, pp. 1054–1068, 1988.
- [3] H. J. Chai, H. C. Liu, Z. Y. Zhang, and Z. W. Xu, "The distribution, causes and effects of damming landslides in China," *Journal of the Chengdu Institute of Technology*, vol. 27, no. 3, pp. 302–307, 2000, in Chinese.
- [4] G. H. Eisbacher and J. J. Clague, *Destructive Mass Movements in High Mountains: Hazard and Management*, Geological Survey of Canada, Ottawa, Canada, 1984.
- [5] A. Pirocchi, "Laghi di sbarramento per frana nelle Alpi: tipologia ed evoluzione," *Atti I convegno Nazionale Giovani Ricercatori in Geologia Applicata*, vol. 93, pp. 128–136, 1992.



- [6] N. Casagli and L. Ermini, "Geomorphic analysis of landslide dams in the Northern Apennine," *Transactions of the Japanese Geomorphological Union*, vol. 20, no. 3, pp. 219–249, 1999.
- [7] J. J. Clague and S. G. Evans, "Formation and failure of natural dams in the Canadian Cordillera," Bulletin 464, Geological Survey of Canada, Ottawa, Canada, 1994.
- [8] H. J. Chai, H. C. Liu, and Z. Y. Zhang, "The catalog of Chinese landslide dam events," *Journal of Geological Hazards and Environment Preservation*, vol. 6, no. 4, pp. 1–9, 1995, in Chinese.
- [9] M. Peng and L. M. Zhang, "Breaching parameters of landslide dams," *Landslides*, vol. 9, no. 1, pp. 13–31, 2012.
- [10] Z. M. Shi, X. Xiong, M. Peng et al., "Risk assessment and mitigation for the Hongshiyuan landslide dam triggered by the 2014 Ludian earthquake in Yunnan, China," *Landslides*, vol. 14, no. 1, pp. 269–285, 2017.
- [11] L. Zhang, T. Xiao, J. He, and C. Chen, "Erosion-based analysis of breaching of Baige landslide dams on the Jinsha River, China," *Landslides*, vol. 16, no. 10, pp. 1965–1979, 2019.
- [12] X. M. Fan, W. Zhan, X. Dong et al., "Analyzing successive landslide dam formation by different triggering mechanisms: the case of the Tangjiawan landslide, Sichuan, China," *Engineering Geology*, vol. 243, pp. 128–144, 2018.
- [13] C. T. Stefanelli, V. Vilimek, A. Emmer, and F. Catani, "Morphological analysis and features of the landslide dams in the Cordillera Blanca, Peru," *Landslides*, vol. 15, no. 3, pp. 507–521, 2018.
- [14] L. Nibigira, H. B. Havenith, P. Archambeau, and B. Dewals, "Formation, breaching and flood consequences of a landslide dam near Bujumbura, Burundi," *Natural Hazards and Earth System Sciences*, vol. 18, no. 7, pp. 1867–1890, 2018.
- [15] L. Ermini and N. Casagli, "Prediction of the behaviour of landslide dams using a geomorphological dimensionless index," *Earth Surface Processes and Landforms*, vol. 28, no. 1, pp. 31–47, 2003.
- [16] G. G. D. Zhou, M. Zhou, M. S. Shrestha et al., "Experimental investigation on the longitudinal evolution of landslide dam breaching and outburst floods," *Geomorphology*, vol. 334, pp. 29–43, 2019.
- [17] S. E. Coleman, D. P. Andrews, and M. G. Webby, "Overtopping breaching of noncohesive homogeneous embankments," *Journal of Hydraulic Engineering*, vol. 128, no. 9, pp. 829–838, 2002.
- [18] Z. Cao, Z. Yue, and G. Pender, "Landslide dam failure and flood hydraulics. Part I: experimental investigation," *Natural Hazards*, vol. 59, no. 2, pp. 1003–1019, 2011.
- [19] L. Schmocker and W. H. Hager, "Plane dike-breach due to overtopping: effects of sediment, dike height and discharge," *Journal of Hydraulic Research*, vol. 50, no. 6, pp. 576–586, 2012.
- [20] J. S. Walder, R. M. Iverson, J. W. Godt, M. Logan, and S. A. Solovitz, "Controls on the breach geometry and flood hydrograph during overtopping of noncohesive earthen dams," *Water Resources Research*, vol. 51, no. 8, pp. 6701–6724, 2015.
- [21] M. W. Morris, M. A. A. M. Hassan, and K. A. Vaskinn, "Breach formation: field test and laboratory experiments," *Journal of Hydraulic Research*, vol. 45, no. 1, pp. 9–17, 2007.
- [22] C. Gregoretto, A. Maltauro, and S. Lanzoni, "Laboratory experiments on the failure of coarse homogeneous sediment natural dams on a sloping bed," *Journal of Hydraulic Engineering*, vol. 136, no. 11, pp. 868–879, 2010.
- [23] G. Pickert, V. Weitbrecht, and A. Bieberstein, "Breaching of overtopped river embankments controlled by apparent cohesion," *Journal of Hydraulic Research*, vol. 49, no. 2, pp. 143–156, 2011.
- [24] L. Schmocker, P.-J. Frank, and W. H. Hager, "Overtopping dike-breach: effect of grain size distribution," *Journal of Hydraulic Research*, vol. 52, no. 4, pp. 559–564, 2014.
- [25] S.-C. Chen, T.-W. Lin, and C.-Y. Chen, "Modeling of natural dam failure modes and downstream riverbed morphological changes with different dam materials in a flume test," *Engineering Geology*, vol. 188, pp. 148–158, 2015.
- [26] X. G. Jiang, J. H. Huang, Y. W. Wei et al., "The influence of materials on the breaching process of natural dams," *Landslides*, vol. 15, no. 2, pp. 243–255, 2018.
- [27] L. Liu, D. Zhong, H. Zhang, and X. Li, "Experimental and numerical study of a landslide dam failure due to overtopping," *Journal of Tsinghua University (Science and Technology)*, vol. 53, no. 4, pp. 583–588, 2013.
- [28] L. Schmocker and W. H. Hager, "Modelling dike breaching due to overtopping," *Journal of Hydraulic Research*, vol. 47, no. 5, pp. 585–597, 2009.
- [29] X. K. Do, M. Kim, H. P. T. Nguyen, and K. Jung, "Analysis of landslide dam failure caused by overtopping," *Procedia Engineering*, vol. 154, pp. 990–994, 2016.
- [30] Y. Zhu, P. J. Visser, J. K. Vrijling, and G. Wang, "Experimental investigation on breaching of embankments," *Science China Technological Sciences*, vol. 54, no. 1, pp. 148–155, 2011.
- [31] N. Liu, Z. L. Cheng, and P. Cui, *Dammed Lake and Risk Management*, Science Press, Beijing, China, 2013, in Chinese.
- [32] Water Resources Department of Sichuan Province China, *Handbook for Calculation of Storm Floods in the Medium and Small Watersheds of Sichuan Province*, Water Resources Department, Chengdu, China, 1984.
- [33] J. Zhang and E. Huang, "Safety analysis of dammed lakes in Wenchuan earthquake," *Advanced Engineering Sciences*, vol. 42, no. 1, pp. 107–112, 2010, in Chinese.
- [34] S. L. Lang, "Forecast on dam-break discharge and hydrologic condition led to overflow burst of landslide dam in Zongqu Gully," *Science Technology and Engineering*, vol. 15, no. 22, pp. 113–117, 2015, in Chinese.
- [35] M. W. Pierce, C. I. Thornton, and S. R. Abt, "Predicting peak outflow from breached embankment dams," *Journal of Hydrologic Engineering*, vol. 15, no. 5, pp. 338–349, 2009.
- [36] V. K. Hagen, "Reevaluation of Design Floods and Dam Safety," in *Proceedings of 14th Congress of International Commission on Large Dams*, Rio de Janeiro, Brazil, 1982.
- [37] S. G. Evans, "The maximum discharge of outburst floods caused by the breaching of man-made and natural dams," *Canadian Geotechnical Journal*, vol. 23, no. 3, pp. 385–387, 1986.
- [38] V. P. Singh and C. A. Quiroga, "A dam-breach erosion model: I. Formulation," *Water Resources Management*, vol. 1, no. 3, pp. 177–197, 1987.
- [39] D. L. Fread, *BREACH: An Erosion Model for Earthen Dam Failures*, National Weather Service, Silver Spring, MD, USA, 1988.
- [40] J. S. Walder and J. E. O'Connor, "Methods for predicting peak discharge of floods caused by failure of natural and constructed earthen dams," *Water Resources Research*, vol. 33, no. 10, pp. 2337–2348, 1997.
- [41] A. L. Rozov, "Modeling of washout of dams," *Journal of Hydraulic Research*, vol. 41, no. 6, pp. 565–577, 2003.
- [42] L. C. V. Rijn, "Sediment pick-up functions," *Journal of Hydraulic Engineering*, vol. 110, no. 10, pp. 1494–1502, 1984.
- [43] D. S. Chang and L. M. Zhang, "Simulation of the erosion process of landslide dams due to overtopping considering

- variations in soil erodibility along depth,” *Natural Hazards and Earth System Science*, vol. 10, no. 4, pp. 933–946, 2010.
- [44] W. Wu, “Simplified physically based model of earthen embankment breaching,” *Journal of Hydraulic Engineering*, vol. 139, no. 8, pp. 837–851, 2013.
- [45] A. M. Osman and C. R. Thorne, “Riverbank stability analysis. I: Theory,” *Journal of Hydraulic Engineering*, vol. 114, no. 2, pp. 134–150, 1988.
- [46] M. Morris, G. Hanson, and M. Hassan, “Improving the accuracy of breach modelling: why are we not progressing faster?,” *Journal of Flood Risk Management*, vol. 1, no. 3, pp. 150–161, 2008.
- [47] Z. Chen, L. Ma, S. Yu et al., “Back analysis of the draining process of the Tangjiashan barrier lake,” *Journal of Hydraulic Engineering*, vol. 141, no. 4, p. 05014011, 2014.



**Hindawi**

Submit your manuscripts at  
[www.hindawi.com](http://www.hindawi.com)

